

Part II. Temperature Measurement of Flames by Means of the Line-Reversal Method

ABSTRACT

Using the theory developed in Part I, flame temperatures for various fireworks compositions have been measured by means of line-reversal of the Na-D lines.

(1) For low flame temperature compositions:

Compositions that contain combustible organic materials (i.e., shellac, rosin, pine root pitch, etc.) are commonly used in ordinary fireworks.

The author prepared various combinations of components to see the influence of oxidizers, fuels, color agents, etc. Temperatures are measured by method 1 from Part I. The result shows that the highest temperature appears at the base of the flame. Generally potassium perchlorate gives higher temperatures than ammonium perchlorate. Potassium nitrate always gives lower temperatures than other oxidizers.

The highest temperature is obtained when the ratio of fuel to oxidizer (potassium perchlorate, ammonium perchlorate or potassium nitrate) is about 1:5. For this ratio, the maximum temperatures obtained are as follows:

Oxidizer	Temperature (K)
Ammonium perchlorate	2,480
Potassium perchlorate	2,520
Potassium nitrate	2,000

(2) For high flame temperature compositions:

Compositions that contain magnesium powder can create a very high flame temperature of more than 2,900 K. Temperatures were measured by method 2 from Part I. In this case the photographic method was applied to measure the intensity of spectral lines, and we obtained temperatures of 2,700–3,000 K, but the accuracy of these data are not as good because of the uncertainties of the photographic method due to the instability of the flame.

I. Introduction

In Part I the author tried to develop theoretically the line-reversal method in preparation for the flame temperature measurement. Although the ordinary, colored-fireworks flame contains solid or liquid particles, it was shown that even in such cases the line-reversal method is adaptable.

Moreover, a plan for the measurement of flame temperatures that are higher than the standard light, using the line-reversal method with Na-D lines was described.

In this paper the practical measurements concerning both cases under the theoretical consideration described in the Part I are reported.

II. Selection of the Standard Light and Its Calibration

For the standard light, which is used for temperature measurement, it is desirable to use a bulb that has a ribbon filament with a small flat surface. However, such a bulb was not available. Therefore, the author used a commercially available 'Spot Light' based on the recommendation of Dr. Ishida.^[6] The bulb had a power of 100 V, 300 W with a six-coiled filament as shown in Photo 1.

The brightness of the light was the highest at the two center coils, and the lowest at the outside coils. When carefully observing one of the coils, the brightness of the inside surface is higher than that of the outside. Namely, the radiated light beams repeatedly reflected each other inside of the coil as if it were in a tube. Therefore, this phenomenon resembles black body radiation and shows that the bulb can measure higher temperatures than the ordinary flat filament generally used.

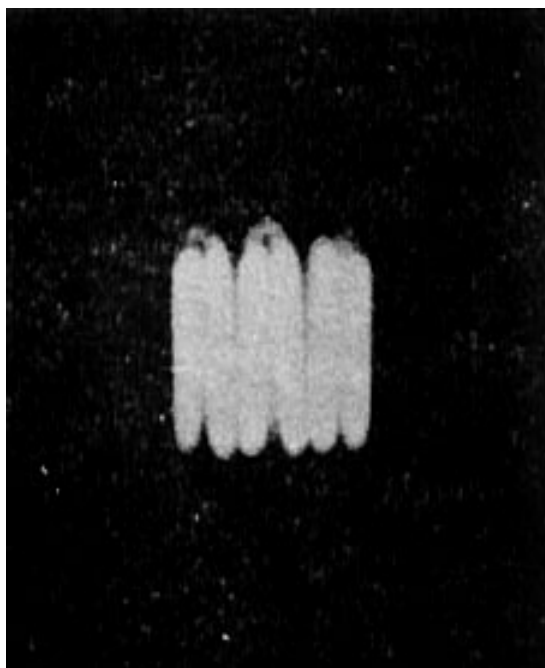


Photo 1. The light from of the standard light.

2.1 The Radiation Pyrometer and Its Calibration

The radiation pyrometer was homemade using an objective lens of 55 mm in diameter with a 110 mm focal length, an ocular lens of 10 mm in diameter with a focal length of 21 mm, and a bulb of 3.5 V. As the filter, a red glass disc wR2 for photographic use was placed in front of the ocular lens assuming that the distance from the object did not affect the data measurements.^[1] The permeability coefficients of the glass disc from the manufacturer's instructions follows:

The Permeability Coefficients $\rho(\lambda)$ of Red Glass wR2.

λ (Å)	$\rho(\lambda)$	λ (Å)	$\rho(\lambda)$
5,800	0.000	6,200	0.835
5,850	0.015	6,250	0.858
5,900	0.050	6,300	0.875
5,950	0.100	6,350	0.888
6,000	0.250	6,400	0.895
6,050	0.500	6,450	0.897
6,150	0.710	6,500	0.900
6,150	0.800	6,550	0.900
		>6,600	0.900

In combination with these and the curve of the international eye sensitivity of the brightness accommodation^[2] and following Wien's equation:

$$E(\lambda, \tau) = c_1 \lambda^{-5} e^{-\frac{c_2}{\lambda \tau}} \quad (1)$$

$$c_1 = 11.906 \times 10^{-6} \text{ erg} \cdot \text{cm}^2 \cdot \text{sec}^{-1}$$

$$c_2 = 1.4387 \text{ cm} \cdot \text{deg}$$

the effective wavelength λ_e for black body temperatures τ were calculated^[3] as follows:

τ (K)	λ_e (Å)
1,273	6,316
2,273	6,259
3,273	6,242
4,273	6,233

For the standard temperature calibration for brightness accommodation, the author used a porcelain electric furnace in place of the black body furnace. The dimensions of the electric furnace were as follows: the internal space was 75 mm in diameter by 115 mm deep (cylindrical in shape); the thickness of the warm wall and bottom was 85 mm. A thermocouple of platinum-rhodium was inserted into the internal space such that it did not touch the inside of the furnace. There was a porcelain lid, which had a 14 mm diameter hole, through which the radiant rays could exit the furnace. While raising the temperature of the furnace, the temperature in the radiant space was not uniform because the bare wire of the electric heater was heated

higher than the wall. Therefore the author raised the temperature to 1200 °C and then switched it off. The calibration of the pyrometer was conducted during the cooling time.

The calibration of the pyrometer was carried out as follows: The small hole was observed through the pyrometer. The brightness of its filament was adjusted so that it coincided with the brightness of the small hole. The electric current of the pyrometer bulb, i mA, and the temperature, denoted by the thermocouple, t °C, was read. These data were recorded and plotted on a graph to obtain an average curve. The largest deviation from the average was 26 °C at 170 mA (Table 1).

Table 1. Calibration Data for Pyrometer.

i mA	160	162	164	166	168	170	172
t °C	712	779	838	892	944	995	1,043

There may be a definite error accompanied with this calibration method. It is thought that the difference between the calibration of this electric furnace and that of the black body furnace is as follows: the radiation loss from the electric furnace is greater than that of black body furnace. However, the thermocouple did not contact the interior surface. If air convection is ignored, the temperatures shown by the thermocouple coincide with that of the temperatures of the black body. To see if the radiation equilibrium is good or not, it was decided to place some small solid material in the electric furnace. When one cannot distinguish this material from the wall of the furnace through the small hole, the radiation is in the black body condition. When calibrating, the brightness of the inner surface and the nichrome wire could not be distinguished.

2.2 Enlargement of the Scale of the Pyrometer

The maximum temperature of the scale obtained from the above calibration was 1,100 °C. For the following use, it must be extended to 1,500 °C. As a base, the values of 170 mA and 995 °C (1,268 K) were used (see Table 1). This is a point near the gold point (1,063 K) and may have the most reliable accuracy for the thermocouple. Therefore, at this point the calibration curve will have high accuracy. The extension method was to use a fan-shaped rotating sector with a direct current bulb and an alternating current bulb.^[4] The results were as follows in Table 2.

Table 2. Extension of the Calibrated Scale.

i mA	170	180	190	200
t °C	1,268	1,470	1,622	1,776

The maximum deviation between the average line and measurement point is 50 °C at 195 mA. There was no difference between the data using direct current and alternating current.

2.3. Calibration of the Standard Light

On the measurement of flame temperatures, the brightness of the image (L_2) at position (F) is the base. The beams come from the standard light (L_1) through the lens (c_1) (see Figure 2 on page 21). Therefore the calibration was carried out by using lens c_1 in the arrangement of measurement taking the distance 1 m from the eye glass of the pyrometer to the position of the image (L_2). With this distance, the deviations, which are caused by the light beam path, are more constant. (The calibration of the pyrometer was carried out in the same way.) To minimize the influence of the spherical aberration of lens c_1 , the distance should be greater. However, the distance should be less when one hopes to regulate the brightness of the standard bulb for the measurement of smaller deviations.

The brightness of the standard light of the pyrometer was not uniform according to the type of the filament because it was a coil type as was that of the standard light used for the line-

reversal measurement process. Therefore, the maximum brightness of the coil was used.

A fan-shaped rotating sector with two blades (25 rps) was placed directly behind the image position to decrease the light intensity, and the scale of the pyrometer was set to 190 mA (1,622 K) or 200 mA (1,776 K). The openings of the fan angle, ϕ , were 72°, 44°, 24°, 8°, 5°, 3°, and 2°. Then the fan was rotated. The brightness of the standard light was adjusted so that it would coincide with that of the filament. At that point, the current and voltage of the standard lamp were read. There was no difference between calibrations in several trials. Therefore, for calibrations, the values of the voltages were used because the voltmeter had a finer scale than the ammeter.

The black body temperatures were calculated using the following formula:^[4]

$$\log \frac{360}{\phi} = 0.4343 \frac{c_2}{\lambda_e} \left(\frac{1}{\tau_o} - \frac{1}{\tau} \right) \quad (2)$$

where τ_o is the base temperature of the pyrometer, and τ is the black body temperature of the standard light. For the value of λ_e , the author used 6,290 Å, which corresponds to the value of a rough estimate for an anticipated average of the temperatures τ_o and τ . A deviation of about 10 Å does not seriously affect the calculation of the value of τ .

The calibration was carried out three times: before, during and after the measurement. The effect of the first calibration showed the highest temperatures; that of the second, the lowest; and that of the third, the middle at every reading of the current meter. This may be caused by stabilizing the filament of the standard light during use (Figure 1).^[3]

For reference, Dr. Ishida's calibration curve, using a spot light as the standard light, is shown.^[6] The bulb used was different from the author's, and it is difficult to compare the effects with those of this paper; however, the inclination of the curve resembles well the result of this calibration.

2.4. Correction of the Calibration Data Considering Wavelength

Considering the results of calculation from equation 2, a value of wavelength $\lambda_e = 6,290$ Å at 1,500 K for the calibration of the standard light was used. However, for the line-reversal method, the Na-D lines, 5,896 and 5,890 Å were used. The tungsten filament is not a gray body, but the emissivity coefficient depends upon the wavelength of the light used. Therefore, the calibration curve with λ_e must be corrected as it was for the curve with λ_e .

The true temperature of the filament is denoted by T , corresponding to black body temperatures τ_e and τ_D , for wavelengths λ_e and λ_D , and the emissivities by $E(\lambda_e, T)$ and $E(\lambda_D, T)$. Here the answer required is the difference between the values of black body temperatures at λ_e and λ_D at the position of the image of the flame. The glass of the bulb and its reflection has an influence on the value. The relations between these items are shown as follows:

$$E(\lambda_e, \tau_e) = g(\lambda_e) \varepsilon(\lambda_e, T) E(\lambda_e, T) \quad (3)$$

$$E(\lambda_D, \tau_D) = g(\lambda_D) \varepsilon(\lambda_D, T) E(\lambda_D, T) \quad (4)$$

where E denotes the intensity of the sample thermal radiation, g the permeability of the bulb glass multiplied by that of the lens, ε the emissivity coefficient for the black body, E the emission intensity of the black body. When one introduces these relations into Wien's equation 1 we have:

$$\frac{1}{\tau_e} = \frac{1}{T} - 2.303 \frac{\lambda_e}{c_2} \log \varepsilon(\lambda_e, T) g(\lambda_e) \quad (5)$$

$$\frac{1}{\tau_D} = \frac{1}{T} - 2.303 \frac{\lambda_D}{c_2} \log \varepsilon(\lambda_D, T) g(\lambda_D) \quad (6)$$

The reflection coefficient of glass is shown as follows, when the beam lines enter the glass perpendicular to the surface, we have, for one surface:

$$R = \left\{ \frac{n(\lambda) - 1}{n(\lambda) + 1} \right\}^2 \quad (7)$$

where $n(\lambda)$ shows the refractive index of the glass to air as a function of the wavelength λ . In

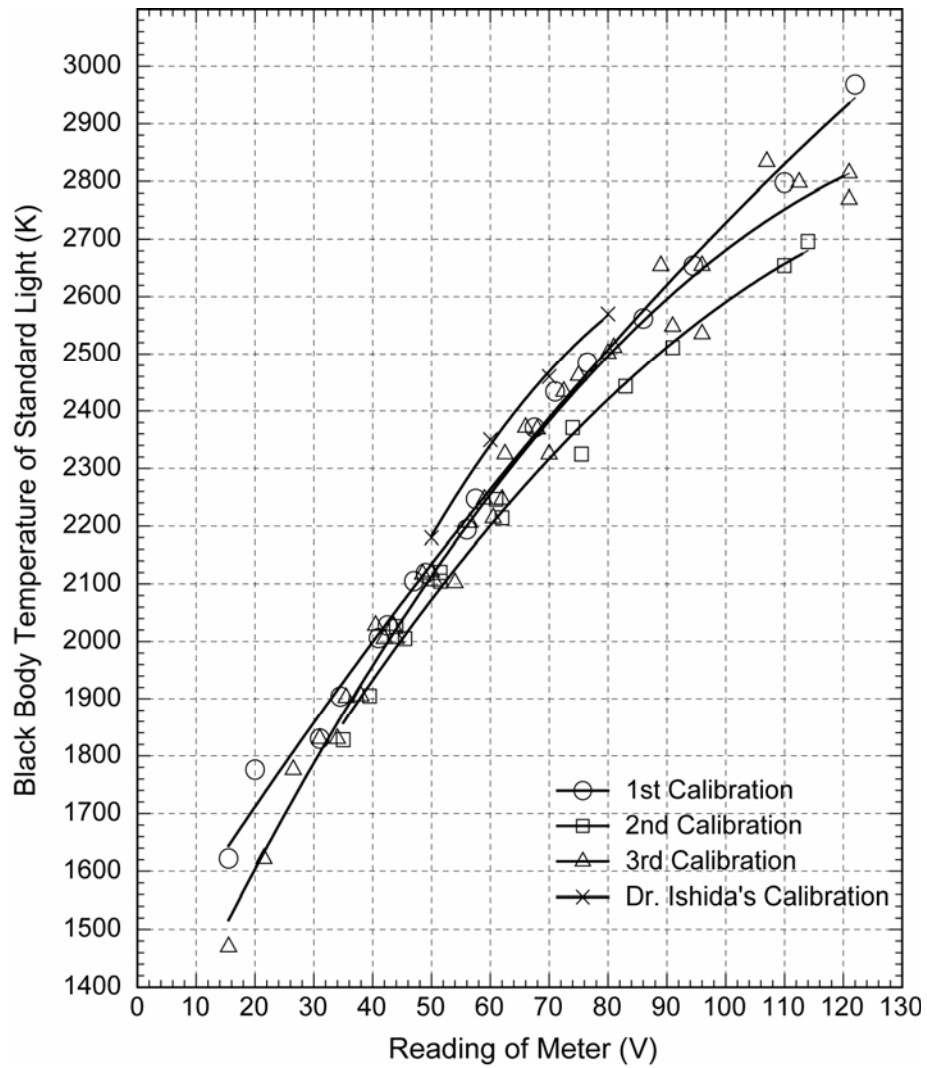


Figure 1. Calibration curves of the standard light.

this case $\lambda_e = 6,290 \text{ \AA}$ and $\lambda_D = 5,890 \text{ \AA}$, and the difference between the two is negligible, so one can use the value $n = 1.52$. Introducing this value to equation 7 we have $R = 0.043$. Therefore, the permeability of one side surface of the glass is calculated as 0.957. There are four surfaces in the beam path, two at L_1 and two at c_1 (i.e., in total 4). Therefore the total permeability is:

$$g(\lambda_e) \doteq g(\lambda_D) \doteq 0.957^4 = 0.839$$

Therefore, we obtain equations 8 and 9 from equations 5 and 6:

$$\frac{1}{\tau_e} = \frac{1}{T} - 0.00009721 \times \log 0.839 \cdot \varepsilon(\lambda_e, T) \quad (8)$$

$$\frac{1}{\tau_D} = \frac{1}{T} - 0.00009433 \times \log 0.839 \cdot \varepsilon(\lambda_D, T) \quad (9)$$

The values of the emissivity coefficient of the ribbon type tungsten filament are shown in Table 3.^[9]

Table 3. The Emissivity Coefficients $\varepsilon(\lambda, T)$ for the True Temperatures T of the Ribbon Type Tungsten Filament.

$$(\lambda_e = 6,290 \text{ \AA}, \lambda_D = 5,890 \text{ \AA})$$

T (K)	$\varepsilon(\lambda_D, T)$	$\varepsilon(\lambda_e, T)$
1,600	0.452	0.457
1,800	0.449	0.453
2,000	0.445	0.450
2,200	0.441	0.446
2,400	0.437	0.443
2,600	0.434	0.439
2,800	0.431	0.436

Introducing these values into equations 8 and 9 we have the values of τ_e , τ_D and the differences $\tau_D - \tau_e$ in Table 4.

Table 4. Black Body Temperatures τ_e, τ_D and $\tau_D - \tau_e$ for the True Temperatures T .^[7]

T (K)	τ_D (K)	τ_e (K)	$\tau_D - \tau_e$
1,600	1,502	1,503	-1
1,800	1,676	1,677	-1
2,000	1,846	1,848	-2
2,200	2,014	2,016	-2
2,400	2,179	2,181	-3
2,600	2,340	2,343	-3
2,800	2,500	2,503	-3

According to Table 4, the calibration curve is usable without correction because the values of $\tau_D - \tau_e$ lie in the range of experimental error. (In this experiment the filament of the standard light was of the coiled type; therefore, the measured temperatures may be nearer the true temperatures and the correction value may be smaller than the values in Table 4.

III. Spectroscope, Installation of Devices and Measurement Operations

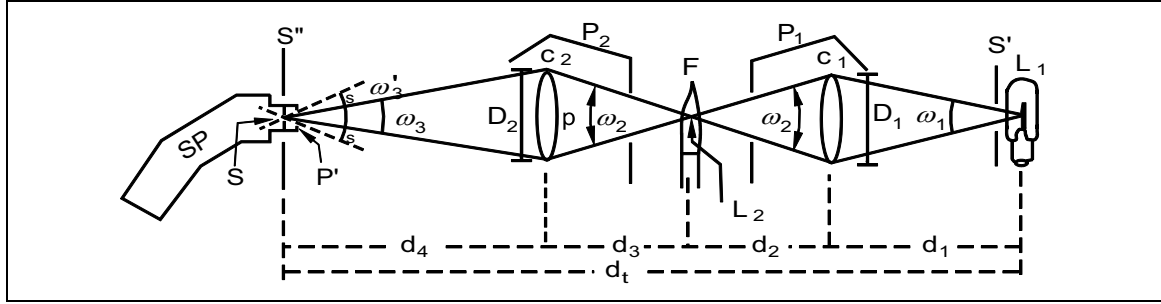
3.1. Dispersion of the Spectroscope

When measuring flame temperatures by means of method 1,^[8] which is based on naked eye observation, the spectroscope should possibly be brighter to minimize the errors, especially if the flame temperatures are low. Therefore, the spectroscope's dispersion (spread of the light beam) should not be very large. When comparing the blackening densities of the dry plate by means of method 2,^[9] a larger dispersion is better for good accuracy, even if the spectroscope is somewhat dark. However, the exposure time should not be very long to avoid a change in state of the flame with time. The dispersions used in the experiment were 60 Å/mm (with three water prisms) for method 1 and 6 Å/mm (with five water prisms) for method 2. The construction of the spectroscope is explained in Part III. (Also see Figure 1a in Part I.)

3.2 Light Path for Measurement

Figure 2 shows the light path for measurement.

The standard light for measurement is not L_1 , but L_2 . Namely, when one sees the light source from p in the direction F and at the solid angle ω_2 , L_2 becomes a light source. Consider when using a light beam of the wavelength λ_i , the energies of the light beams that are emitted from the first light source L_1 in the unit area, in the unit solid angle, and in the unit time is denoted as $E(\lambda_i, \tau_1)$. The total radiation energy per unit time is $E(\lambda_i, \tau_1) \omega_1 s_1$, where s_1 is the total radiation area of the light source L_1 , and the emission surface is a uniform flat surface perpendicular to the axis of the light beam path. The emission surface produces the radiation uniformly (Assumption 1), and the directions of the light beams are uniform in the solid angle ω_1 (Assumption 2). As stated in 2.4, the light beams which pass through the lens c_1 are partially reflected at both sides of the lens. The absorption



L ₁	First standard light	p	Center of second collection lens c ₂
L ₂	Second standard light (the image of L ₁)	P'	Protection glass for slit.
F	Flame	P ₁ , P ₂	Lens Protector
c ₁	First collection lens	ω	Angles of image
c ₂	Second collection lens	s	Light inlet angle
S	Slit	d	Distance between equipment
S'	Shading of random light	D ₁ , D ₂	Diameter of lenses
S''	Screen for making image of the flame	SP	Spectroscope

Figure 2. Installation of the devices for temperature measurement.

of the lens glass is negligible when using visible rays.

When light energy is emitted from the second light source L₂ in the unit solid angle and unit time having a wavelength λ_i, denoted as E(λ_i, τ₂), the total energy is under the same assumption in the unit time is E(λ_i, τ₂) ω₂s₂, where s₂ is the total radiation area of the light source L₂. Expressing the reflecting coefficient with R_{s₁}(λ_i), the relation of energy is

$$E(\lambda_i, \tau_2) \omega_2 s_2 = \{1 - R_{s_1}(\lambda_i)\} E(\lambda_i, \tau_1) \omega_1 s_1$$

Accordingly, we have:

$$E(\lambda_i, \tau_2) = \frac{\omega_1 s_1}{\omega_2 s_2} \{1 - R_{s_1}(\lambda_i)\} E(\lambda_i, \tau_1) \quad (10)$$

From the relation of optical geometry, we have:

$$\omega_1 s_1 = \omega_2 s_2 \quad (11)$$

Therefore

$$E(\lambda_i, \tau_2) = \{1 - R_{s_1}(\lambda_i)\} E(\lambda_i, \tau_1) \quad (12)$$

Namely, the brilliancy of the light source L₂ is less than that of L₁ based on the quantity of re-

flection by the lens c₁. The brilliancy of the light source is independent of the size of the lens, and the distance from the standard light L₁ on the image L₂ to the lens. Concerning the lens c₂ the same relation as above is adaptable as:

$$E(\lambda_i, \tau_3) = \{1 - R_{s_2}(\lambda_i)\} E(\lambda_i, \tau_2) \quad (13)$$

Therefore, the brilliancy of the second light source at the slit decreases due to the reflections of the lens c₂ and has no influence on other conditions.

Therefore to decide the dimension of the lenses, their focal lengths, and the distance from the source of the light to the image, the following conditions should be considered.

(1) To meet assumption 1, one should use the middle part of a light source, which has a wider surface.

(2) To meet assumption 2, the diameter of each lens c₁ and c₂ should not be very large for the distance d₁ or d₂. Therefore the focal length of lens c₁ or c₂ should be larger.

(3) To obtain the highest accuracy, the spectroscope should be very bright. Therefore, the distances d₂ and d₃, the focal length, and the

diameter of the lenses were determined as follows:

Lens c_1	possibly a large diameter,
Distance d_1	possibly smaller to enlarge the angle ω_1
Lens c_2	the angle ω_3 coincides with the angle of visible range of the spectroscope, and is perfectly covered by the solid angle ω_2 .

(4) The size of the image of light source L_2 on the slit (on the screen S') should, if possible, be large, and the part of the image of uniform brightness should be aimed at the slit S . In the case of the coiled filament, the most brilliant part should be aimed at the slit.

(5) The chromatic aberration of the lenses does not interfere with the measurement.

(6) Spherical aberration causes a dispersion of the image, decreases its brightness, and the axis of the light path does not coincide with that of the pyrometer. It increases errors during calibration. Therefore, the calibration should be carried out with a pyrometer having a small object lens at a more distant position in the optical axis. However, such a method decreases the accuracy of the calibration.

(7) The flame has a thickness; therefore, the measured area is shown as in Figure 3. The value obtained is an average of that portion within the solid angle ω_2 . Therefore, to obtain accurate values, the solid angle ω_2 should be small.

In the above conditions, some contradict each other; however, they are selected based on the purpose of the experiment, the availability of materials, the location of the experiment, the extent of danger, the protection of devices, etc.

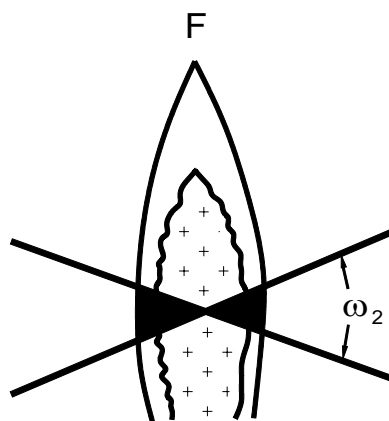


Figure 3. The influences of the thickness of the flame.

3.3 Installation of Devices and Operation

The most important point was how to avoid wind and smoke.

The standard light L_1 , lens c_1 , and lens c_2 were arranged on a long wooden frame. A burning chamber made of tin plates, which protected the flame from wind, was set between c_1 and c_2 . The frame of these instruments was set outdoors so that the wind and smoke did not interfere with the measurement. The light beams from the burning sample and the standard light were fed indoors into the spectroscope through a small window in the measuring room. The sample holder was a tube that was attached to a solid stand, which could be adjusted so that the position of the burning surface of the sample moved up and down during the burning of the sample. A screen was set directly in front of the slit to see the image of the flame and to detect what part of the flame was introduced into the slit. A scale was marked on the screen to see the position of the sample flame. The distances were as follows: $d_1 = 575$ mm, $d_2 = 305$ mm, $d_3 = 310$ mm, $d_4 = 450$ mm. The focal length and the diameter of the lenses were: $f_1 = 195$ mm, $f_2 = 174$ mm, $D_1 = 81$ mm, $D_2 = 74$ mm.

The outdoor operations were as follows: Adjust the sample holder to produce the image of the standard light in the middle of the flame. Adjust the position of the wooden frame so that the maximum intensity of the filament image

from the standard light passed through the slit. During the measurement the position of the image of the filament is somewhat removed and the position is often moved by oscillation. Therefore, the position was checked just before each measurement. The level of the sample was regulated by the handle of the holder so that the temperature of the aimed point of the flame passed through the slit. The length of the tube became shorter and shorter, and attention to this was especially important. On the burning of the samples, protection of the slit and lenses was very important.

IV. Preparation of Samples

4.1 Chemicals

The details are described in Part III; however, the chemicals selected were of as high quality as possible from samples used for spectral analysis.

These were dried at 60–110 °C before mixing. However, a good quality magnesium powder was not available; so a commercial grade was used. It was analyzed as 75.72% Mg, 24.28% Al with no insoluble matter in the HCl solution.

4.2 Sample Compositions and the Specimens

The sample compositions were limited to those that were useful for the spectral analysis of the flames (Tables 6, 9, 10, 11, and 12).

Each mixture was loaded firmly by hand into a double wound brown paper tube.^[10] The dimensions of a completed sample specimen was 10 mm in diameter and 98 mm long. For ignition, a piece of black match was inserted and attached to the top by pasting with thin paper.

V. Temperature Measurement of Low Temperature Flames and Examination of the Results

5.1 The Condition of the Flames, Flame Temperature Data, and Measurement Errors

Examples of low temperature flames are shown in Photo 2. The flames were not as stable as those of a gas burner; however, they were fairly stable. The results are shown in Figures 4–9. The symbols used are:

Δ	loading density, g/cc
v	burn rate, mm/sec
l	length of flame, cm
d	distance from the base to the measuring point of the flame, cm

To determine the temperature, calibration curve 3 was used (Figure 3). The measured data in Figures 4–9 are the average values of four

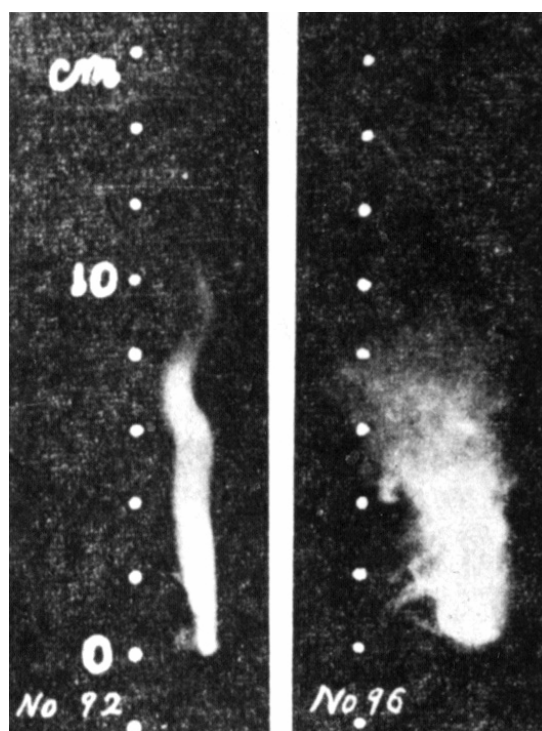


Photo 2. Flames from No. 92, ammonium perchlorate composition and No. 96, potassium perchlorate composition.

time trials at the center of flame.

The probability errors calculated with equation 14 are shown in Table 5.

$$r_T = 0.6745 \sqrt{\frac{\sum e^2}{n-1}} \quad (14)$$

Where r_T is the probability error for the measured values, e is the deviation of each value from the average, and n is the number of the values.

During the measurement, adjusting the brightness of the filament of the standard light was relatively easy. Therefore, errors come mainly from the instability of the flame. Table 5 shows that the position of the most stable points lie 2 cm from the flame base.

Table 5. Probability Errors of Measured Flame Temperature Data r_T (Low Temperature Flames)

τ (K) \ d (cm)	1.0	2.0	3.0	4.0
1,800–2,000	66.7°	28.7°	62.7°	92.9°
2,000–2,200	43.4°	27.1°	33.9°	61.0°
2,200–2,400	44.6°	34.1°	45.1°	36.3°
2,400–2,600	32.3°	25.5°	28.3°	30.9°
2,600–2,800	29.9°	32.5°	—	—

Note: K = Flame temperature in absolute units, Kelvin

d (cm) = distance from the base of the flame along the center line of the flame to the objective point.

5.2 Distribution of Temperatures in a Flame

Figures 4–9 show that temperatures along the center line of the flame were different based on the type of oxidizer, fuel, etc. Generally, temperatures were highest near the base of the flame and decreased along the length of the flame.

5.3 Influence of Oxidizer Type and Mixing Ratios

Flame temperatures were measured with compositions in Table 6. The results are shown in Figures 4 and 5.

Table 6. Sample Mixtures To Study the Effect of Oxidizers, Fuels and Mixing Ratios.

Composition (1)	%
Ammonium perchlorate	x
Shellac	y
Sodium oxalate	10

No.	$x\%$	$y\%$	$\Delta(\text{g/cm}^3)$	υ (s)	ℓ (cm)
90	65	25	1.15	0.91	12–19
91	70	20	1.15	0.99	<13
92	75	15	1.15	1.07	10–12
93	80	10	1.17	0.93	7–9

Composition (2)	%
Potassium perchlorate	x
Shellac	y
Sodium oxalate	10

No.	$x\%$	$y\%$	$\Delta(\text{g/cm}^3)$	υ (s)	ℓ (cm)
94	65	25	1.33	1.04	17–19
95	70	20	1.30	1.35	12–13
96	75	15	1.33	1.50	<9
97	80	10	1.30	1.30	6–8

Composition (3)	%
Potassium chlorate	x
Shellac	y
Sodium oxalate	10

No.	$x\%$	$y\%$	$\Delta(\text{g/cm}^3)$	υ (s)	ℓ (cm)
98	65	25	1.14	2.46	24–26
99	70	20	1.13	2.34	<20
100	75	15	1.11	2.40	<12
101	80	10	1.17	1.86	5–8

Table 6. Sample Mixtures To Study the Effect of Oxidizers, Fuels and Mixing Ratios (Continued).

Composition (4)	%
Potassium nitrate	x
Shellac	y
Sodium oxalate	10

No.	x%	y%	$\Delta(\text{g/cm}^3)$	ν (s)	ℓ (cm)
191	65	25	1.29	1.16	—
192	70	20	1.35	1.20	13–14
193	75	15	1.43	2.00	4–8
194	80	10	1.43	—	—

Composition (5)	%
Barium nitrate	x
Shellac	y
Sodium oxalate	10

No.	x%	y%	$\Delta(\text{g/cm}^3)$	ν (s)	ℓ (cm)
198	65	25	1.05	1.37	12–13
199	70	20	1.11	1.26	9–12
200	75	15	1.09	1.37	9–10
201	80	10	1.18	1.60	7–9

The loading density was the highest with potassium perchlorate or potassium nitrate, the value was about 1.3 g/cc, and 1.1–1.2 g/cc with ammonium perchlorate and potassium chlorate. The burn rate was greatest for potassium chlorate and decreased in the order of potassium perchlorate, potassium nitrate, and ammonium perchlorate. However, the potassium nitrate composition burned with so much ash (It had to be viewed in a special way). Therefore, it may be difficult to compare with the others.

The maximum flame temperature was 2,518 K with potassium perchlorate and decreased in the order of ammonium perchlorate and potassium chlorate. With potassium nitrate the temperature was lowest, 2,000 K. This might explain the poor ability of color production with potassium nitrate. No relationship was found between flame temperature and oxygen balance.

The temperature gradation from the base of a flame was smallest with the potassium chlorate composition; and potassium nitrate compositions have the same tendency. Other compositions showed steeper gradation and showed a temperature decrease of 50–80 °C per 1 cm of flame length. Barium chlorate compositions showed almost the same characteristics as the potassium chlorate compositions.

The fuel/oxidizer ratio had a great influence on flame temperatures. When the fuel, shellac, was increased, the temperatures of the flame increased to the maximum when the ratio of fuel/oxidizer was 1:5, and the temperatures fell with decreasing ratios.

The relationship of the deficiency of oxygen in the flame and flame temperatures was unknown because the reaction mechanism in the flame was unknown. However, on the assumption of perfect oxidation of the fuels, the quantities of insufficient oxygen are calculated in Tables 7 and 8.

Table 7. Calculated Values of Sufficient or Deficient Oxygen Values for a 100 g Mixture of CO₂ Oxidation.

Composition	%
Oxidizer	x
Shellac	y
Sodium oxalate	10

Oxidizer	Oxidizer (%)			
	65	70	75	80
NH ₄ ClO ₄	-33.6	-20.7	-7.9	+4.9
KClO ₄	-25.6	-12.2	+1.3	+14.7
KClO ₃	-30.2	-17.1	-4.0	+9.1
KNO ₃	-29.9	-16.8	-3.7	+9.4
Ba(ClO ₃) ₂ ·H ₂ O	-36.3	-23.7	-11.0	+1.6

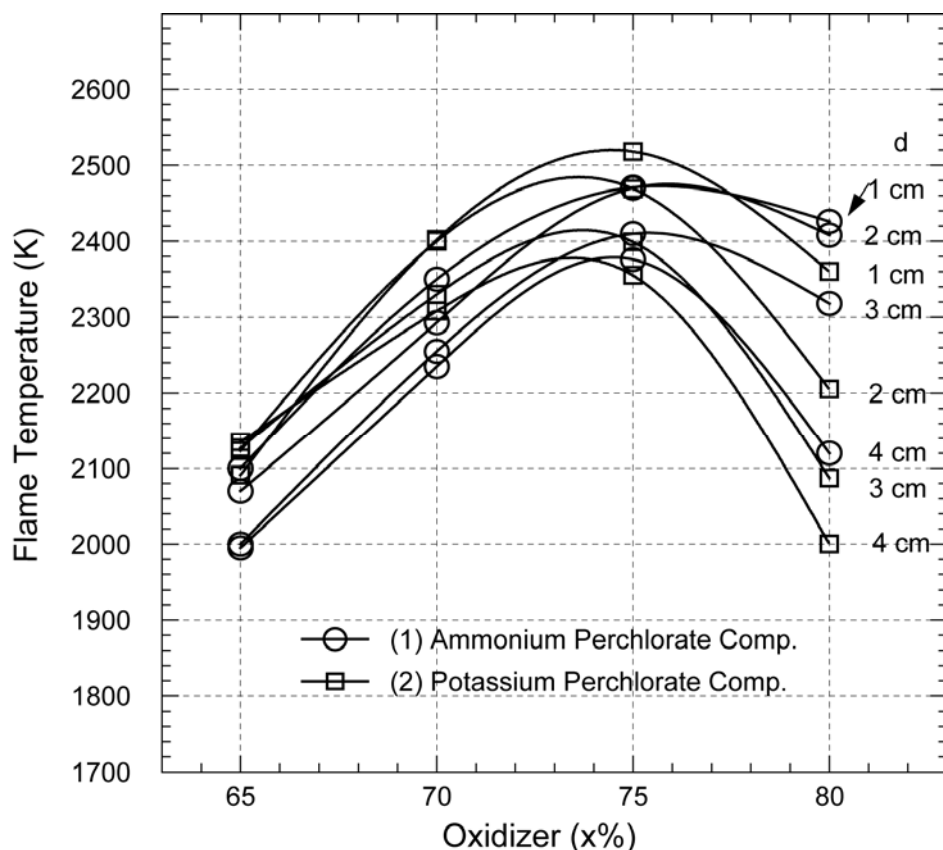


Figure 4. Flame temperatures: the effects of oxidizers, fuels and mixing ratios (1).

Table 8. Calculated Values of Sufficient or Deficient Oxygen Values for a 100 g Mixture of CO Oxidation.

Composition	%
Oxidizer	x
Shellac	y
Sodium oxalate	10

Oxidizer	Oxidizer (%)			
	65	70	75	80
NH_4Cl_4	-11.5	+3.1	+5.4	+13.8
KClO_4	-3.6	+5.5	+14.5	+23.5
KClO_3	-8.1	+0.6	+9.3	+14.9
KNO_3	-7.8	+0.9	+9.6	+18.3
$\text{Ba}(\text{ClO}_3)_2 \cdot \text{H}_2\text{O}$	-14.2	-6.0	+2.2	+10.4

According to Tables 7 and 8, 75% oxidizer, which gave the highest flame temperature, showed slight oxygen deficiencies except for

potassium perchlorate when CO_2 oxidation took place. However, for CO oxidation, the quantity of oxygen was rich enough to react.

5.4 Influence of the Type of Fuel

Flame temperatures were measured using compositions in Table 9. Together with the results using compositions in Table 6, we see that the flame temperatures were different for the various types of fuel: shellac, colophony, pine root pitch, or wood meal. With ammonium perchlorate pine root pitch gave the highest temperatures, followed by shellac and colophony. However, with potassium perchlorate, pine root pitch gave higher temperatures than shellac. The 1 gram oxygen equivalent value of the fuels are: for colophony, 2.565 grams; for shellac, 2.261 grams; for pine root pitch, 2.376 grams; and for wood meal, 1.370 grams. However, this order does not coincide with the order of temperature values (Figure 6).

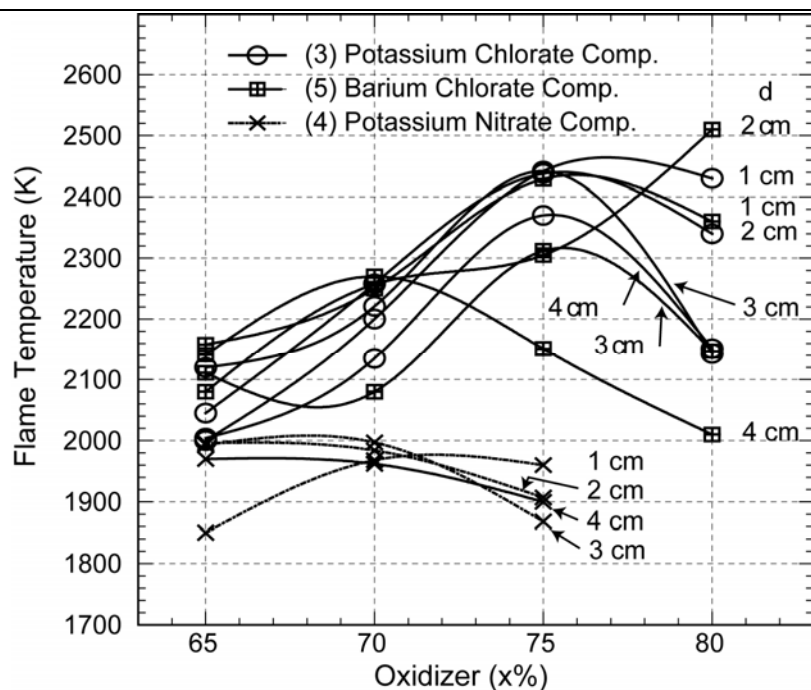


Figure 5. Flame temperatures: the effects of oxidizers, fuels and mixing ratios (2).

Table 9. Effect of Fuel Type.

Composition (6)	%
Ammonium perchlorate	75
Fuel	15
Sodium oxalate	10

No.	Fuel	$\Delta(\text{g}/\text{cm}^3)$	v (s)	l (cm)
102	Colophony	1.06	0.66	6–9
103	Pine root pitch	1.13	1.98	16–21
104	Wood meal	0.96	0.86	<5

Composition (7)	%
Potassium perchlorate	75
Fuel	15
Sodium oxalate	10

No.	Fuel	$\Delta(\text{g}/\text{cm}^3)$	v (s)	l (cm)
105	Colophony	—	1.07	10–12
106	Pine root pitch	1.33	3.00	10–12
107	Wood meal	1.26	1.34	3–5

Composition (8)	%
Potassium nitrate	75
Fuel	15
Sodium oxalate	10

No.	Fuel	$\Delta(\text{g}/\text{cm}^3)$	v (s)	l (cm)
195	Colophony	0.99	—	no flame
196	Pine root pitch	1.13	2.56	—
197	Wood meal	0.95	—	did not burn

Composition (9)	%
Barium chlorate	75
Fuel	15
Sodium oxalate	10

No.	Fuel	$\Delta(\text{g}/\text{cm}^3)$	v (s)	l (cm)
202	Colophony	1.38	half burnt	—
203	Pine root pitch	1.41	3.24	—
204	Wood meal	1.19	0.66	—

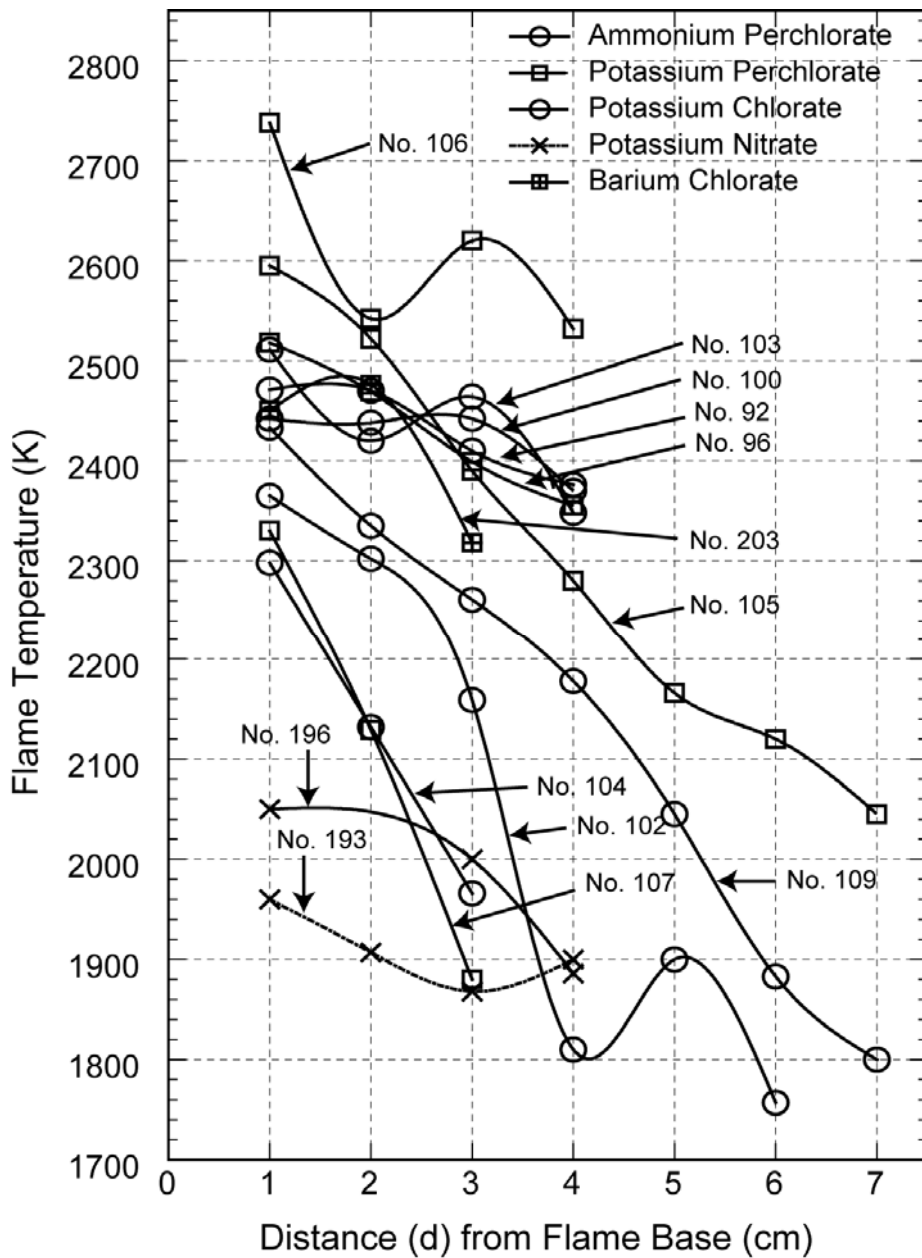


Figure 6. The effect of types of fuel with various oxidizers.

5.5 Effects of Various Color Agents

Flame temperatures were measured with compositions in Table 10 and the results are shown in Figures 7–9.

Table 10. Effects of Color Agents.

Composition (10)	%
Ammonium perchlorate	71
Shellac	14
Color agent	10
Sodium oxalate	5

No.	Color agent	$\Delta(\text{g/cm}^3)$	ν (s)	l (cm)
108	Strontium carbonate	1.16	0.78	6–8
109	Strontium oxalate	1.13	0.79	8–10
110	Strontium chlorate	1.19	0.96	8–10
111	Strontium nitrate	1.19	1.07	9–11
112* ¹	Sodium carbonate	1.13	0.94	5–8
113* ¹	Sodium chloride	1.22	1.08	10–13
114* ¹	Sodium bicarbonate	1.19	0.74	8–10
115	Barium carbonate	1.17	0.80	9–11
116	Barium oxalate	1.13	0.95	10–12
117	Barium chlorate	1.20	0.93	10–12
118	Barium nitrate	1.24	0.98	11–13
119	Basic copper carbonate	1.13	2.28	15–18
120	Copper oxalate	1.12	1.18	18–21
121	Copper sulfate with waters of hydration	1.19	1.00	14–21
122	Paris green	1.13	1.30	17–20
123	Copper arsenite	1.06	1.51	16–22
124	Copper powder 10%	1.19	2.56	17–20
125* ²	Copper powder 5%	1.21	2.16	16–20

Note *¹: This composition was a mixture of 75% ammonium perchlorate, 15% shellac, and 10% color agent.

*²: 5% copper powder means 95% in total ratios.

Table 10. Effects of Color Agents (Continued).

Composition (11)	%
Potassium perchlorate	71
Shellac	14
Color producing agent	10
Sodium oxalate	5

No.	Color agent	$\Delta(\text{g/cm}^3)$	ν (s)	ℓ (cm)
126	Strontium carbonate	1.28	1.37	9–10
127	Strontium oxalate	1.32	1.07	7–9
128	Strontium nitrate	1.33	1.63	4–6
169* ¹	Sodium carbonate	1.41	1.13	8–10
170* ¹	Sodium chlorate	1.43	1.14	4–6
171* ¹	Sodium bicarbonate	1.41	0.96	9–11
137	Barium carbonate	1.35	1.35	8–10
138	Barium oxalate	1.33	1.32	9–11
139	Barium chloride	1.31	1.26	9–11
140	Barium nitrate	1.31	1.35	9–10
129	Paris green	1.31	1.92	6–9
130	Copper arsenite	1.31	2.00	8–10
131	Copper powder 10 %	1.28	1.76	12–15
132* ²	Copper powder 5 %	1.23	1.83	9–12
172	Basic copper carbonate	1.33	1.19	10–14
173	Copper oxalate	1.04	1.16	12–14
174	Copper sulfate with waters of hydration	1.31	1.67	3–5

Note : The symbols *¹ and *² are the same as above table.

Composition (12)	%
Ammonium perchlorate	x
Potassium perchlorate	y
Barium nitrate	z
Shellac	15
Sodium oxalate	10

No.	x%	y%	z%	$\Delta(\text{g/cm}^3)$	ν (s)	ℓ (cm)
133	—	60	15	1.31	1.16	9–12
134	—	45	30	1.32	1.02	12
135	60	—	15	1.25	0.57	5–6
136	45	—	30	1.31	0.62	4–5

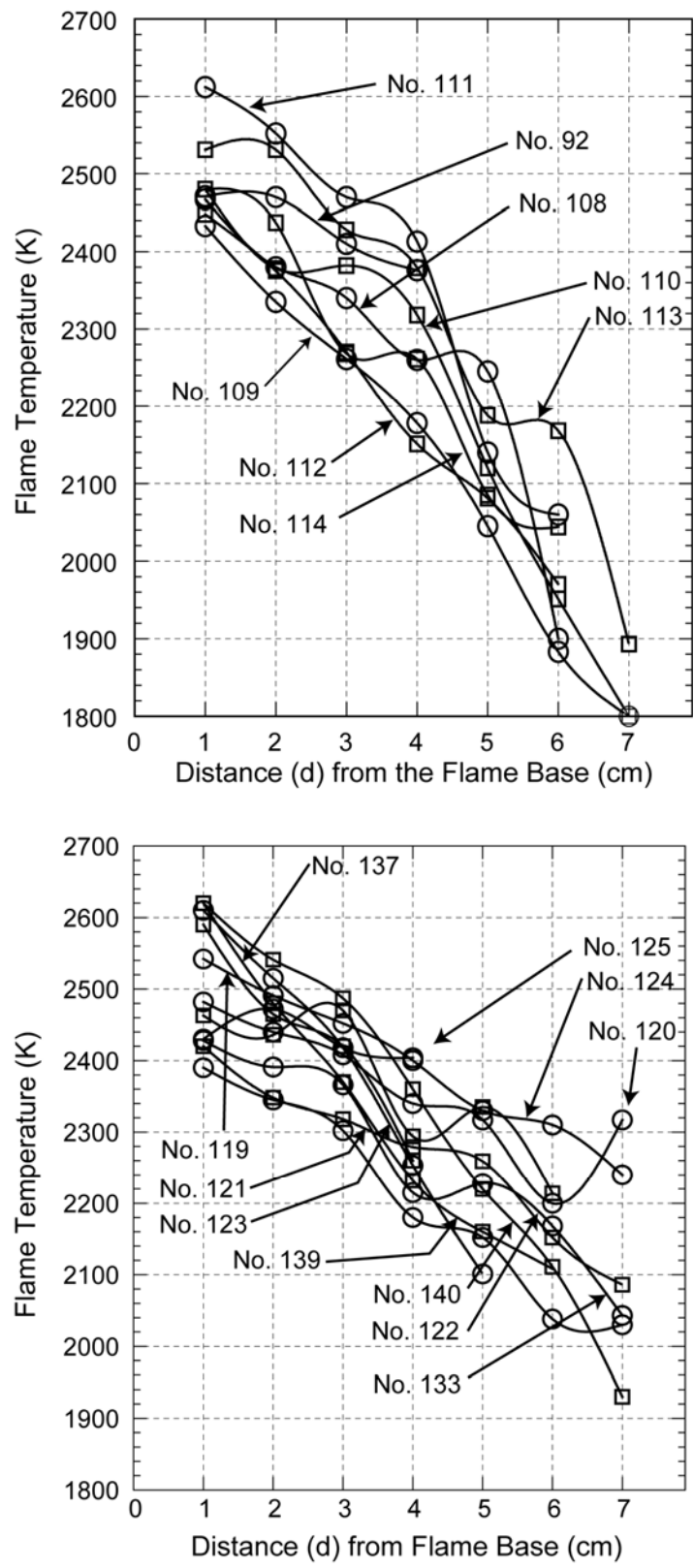


Figure 7. Flame temperatures with compositions of ammonium perchlorate and various fuels.

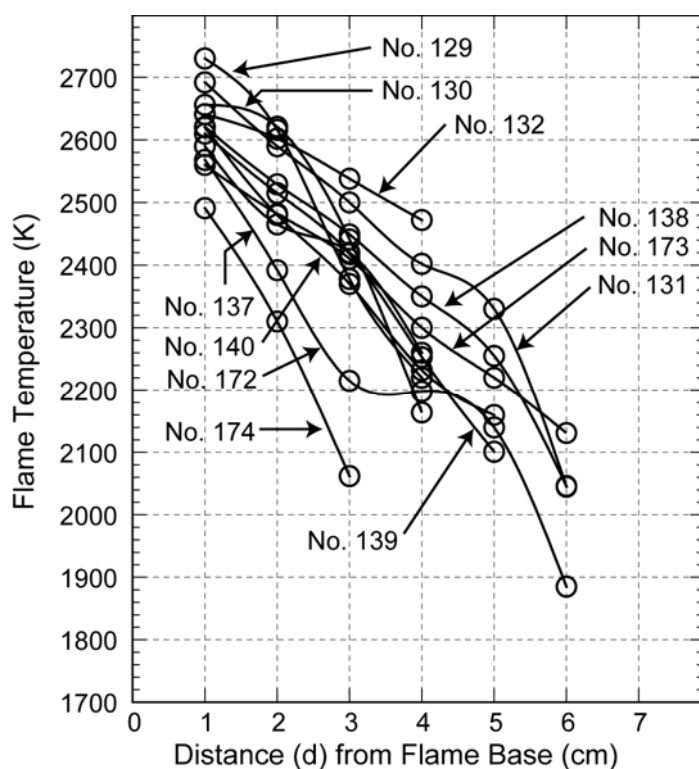
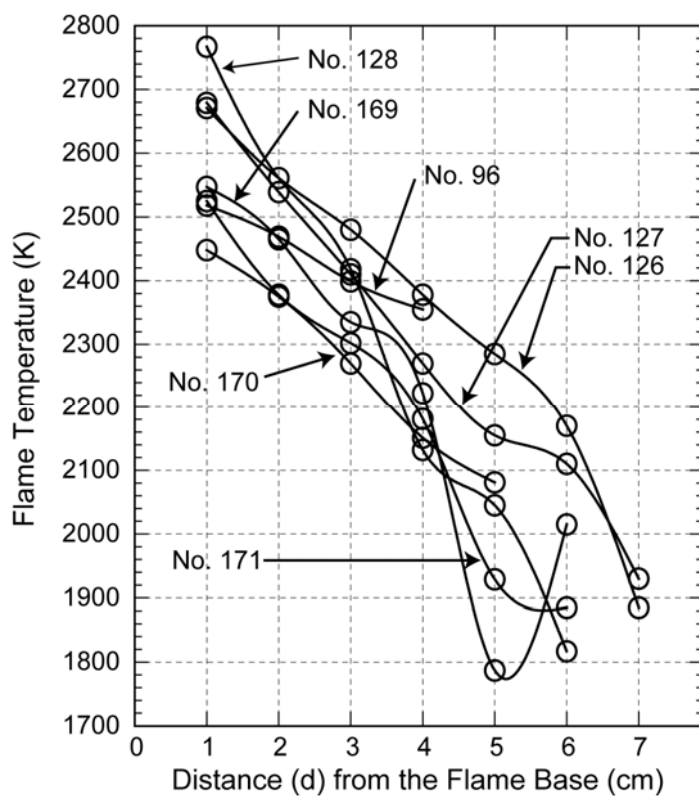


Figure 8. Flame temperatures with potassium perchlorate and various fuels.

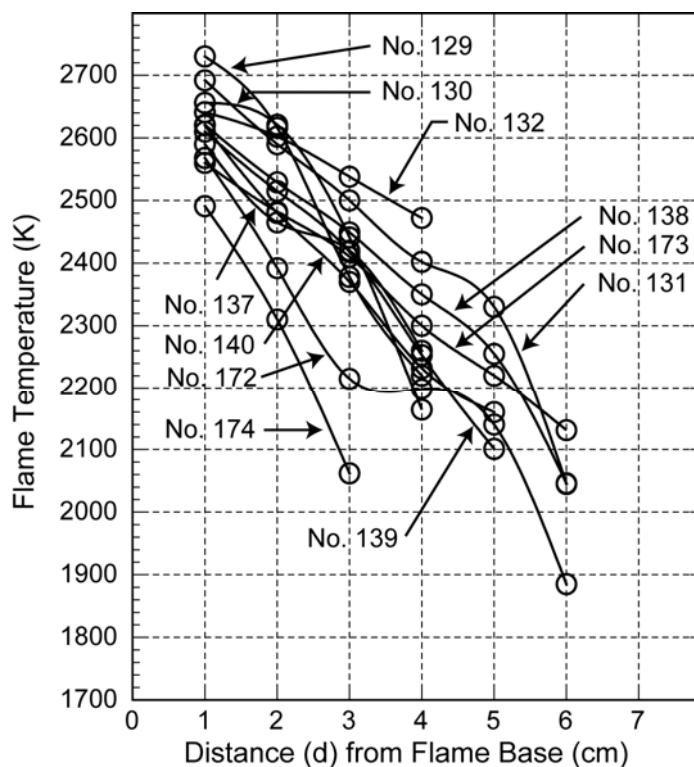


Figure 9. Flame temperatures with mixtures that contain potassium perchlorate, ammonium perchlorate and barium nitrate.

(1) Red color agents (strontium salts)

When using ammonium perchlorate as the oxidizer, strontium nitrate gave temperatures of 100–200 °C higher than other strontium salts. The other strontium salts: chloride, oxalate and carbonate did not show significant differences from each other. When using potassium perchlorate as the oxidizer, strontium nitrate gave higher temperatures than strontium carbonate at the base of each flame. However, in general, one could not find significant differences between the two.

Strontium carbonate produced slightly higher temperatures than strontium oxalate.

(2) Yellow color agents (sodium salts)

When using ammonium perchlorate, sodium chloride gave the highest temperatures of all, with sodium carbonate and sodium bicarbonate about the same. The difference between the chloride and the other sodium salts was about 100 °C.

When using potassium perchlorate as the oxidizer, the gradation of temperatures over the flame length were slightly smaller than with the other oxidizers.

(3) Green color agents (barium salts)

When using ammonium perchlorate, barium nitrate gave higher temperatures than the other oxidizers. The other barium salts, chloride, oxalate, and carbonate had about the same effect. The difference in temperatures between the effect of the nitrate and the others was about 100 °C.

When using potassium perchlorate, the temperature effects were almost the same for each color agent.

(4) Blue color agents (copper salts or copper powder)

Using either ammonium perchlorate or potassium perchlorate the temperature differences were considerable along the flame length among the color agents: 150 °C with ammonium perchlorate and 200 °C with potassium perchlorate. With both oxidizers, copper sulfate with waters of hydration gave the lowest temperatures and copper powder gave the highest. Other blue color agents did not show any special tendency with respect to the type of oxidizer. Paris green and copper arsenite gave lower temperatures with ammonium perchlorate than with potassium perchlorate. The case for basic copper carbonate was the opposite. Copper oxalate always gave higher temperatures.

(5) The effect of mixing ratios of barium nitrate and other oxidizers

This effect will be considered when making green flames (Figure 9). In general potassium perchlorate gave higher temperatures than ammonium perchlorate, and the effects of the mixing ratio of the composition also were larger with potassium perchlorate than with ammonium perchlorate. In both cases the smaller the quantity of barium nitrate, the lower the flame temperature.

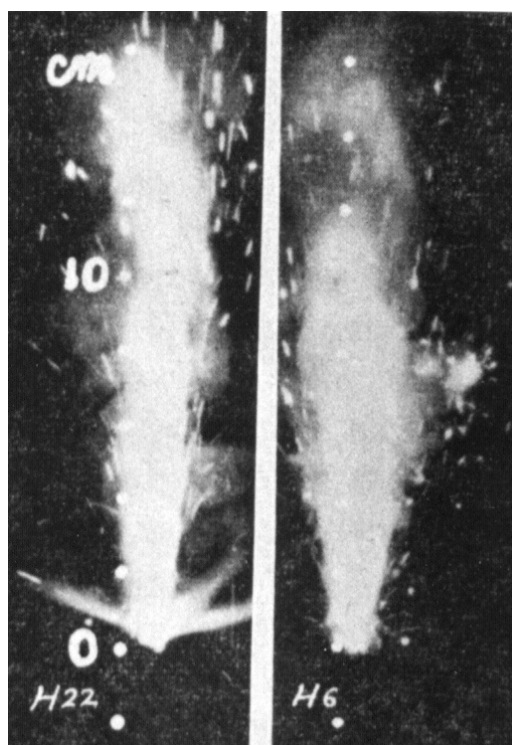


Photo 3. High temperature flames: H22, from an ammonium perchlorate composition and H6, from a potassium perchlorate composition.

VI. Measurements with High Temperature Flames and Discussion of the Results

6.1 Conditions of Flames and Method of Measurement

Examples of high temperature flames are shown in Photo 3. The temperature measuring point was 1 cm from the flame base where it was brightest.

The flame temperatures were measured by method 2 (see Part I). Namely, temperatures of the standard light were changed in four steps and at each step the Na-D lines and neighboring parts of the spectrum were photographed. It was necessary to prepare a characteristic curve of sensitivity of the dry plate that showed the relationship of exposure time and blackening density, from which one could know the relationship of the blackening density to light energy.

(Light energy is proportional to the exposure time on the dry plate.)

The characteristic curve of the dry plate was obtained as follows. Light beams were introduced into the spectroscope with a 0.4 mm wide slit and the dry plate was exposed for $2n$ seconds, where $n = 1, 2, 3, 4 \dots$. Then blackening densities for each image part of the Na-D lines and its neighbors were measured and recorded with the exposure time, and with the resulting curve of n vs. δ , where δ is the blackening density.

The blackening density of the image of the dry plate was obtained as follows. Light beams from the filament of a spot light bulb for photographic use were collected with a 0.4 mm wide slit on an image part of the dry plate, the beams which passed the slit were received by a selenium photometer. The light intensity was measured as the value I . Then a blackening density of no image was measured by the same device as the value I_o . Then the δ value of blackening density δ was obtained as follows:

$$\delta = \log_{10} \frac{I_o}{I} \quad (15)$$

For this method, photographs were used to measure the intensities of the inlet light beams. Small errors might accompany the data at the measurements. However, the errors might be larger than expected, because the stability of high temperature flames was lower than that of low temperature flames.

6.2 Data of the Measurement

The data are shown in Tables 11 and 12. The black body temperatures were changed in four steps: $\tau_1 = 2,380$ K, $\tau_2 = 2,490$ K, $\tau_3 = 2,595$ K, $\tau_4 = 2,690$ K. T is the true temperature of the flame (K).

Table 11. The Effects of the Types of Oxidizer and Mixing Ratios.

Composition (13)	%
Potassium perchlorate	x
Magnesium	y
Shellac	10

No.	$x\%$	$y\%$	$\Delta(\text{g/cm}^3)$	ν (s)	T (K)
H 5	60	30	1.33	2.42	2,830
H 6	45	45	1.22	3.25	2,830
H 7	30	60	1.14	6.62	2,740
H 8	15	75	0.97	6.96	2,730

Composition (14)	%
Potassium nitrate	x
Magnesium	y
Shellac	10

No.	$x\%$	$y\%$	$\Delta(\text{g/cm}^3)$	ν (s)	T (K)
H 9	60	30	1.14	1.90	2,775?
H10	45	45	1.01	3.37	2,725?
H11	30	60	1.01	6.62	2,825?
H12	15	75	0.93	did not burn	

Composition (15)	%
Ammonium perchlorate	x
Magnesium	y
Shellac	10

No.	$x\%$	$y\%$	$\Delta(\text{g/cm}^3)$	ν (s)	T (K)
H21	60	30	1.08	2.41	2,950?
H22	45	45	1.06	4.47	2,875
H23	30	60	1.01	6.23	?
H4	15	75	0.96	9.25	—

Table 11. The Effects of the Types of Oxidizer and Mixing Ratios (Continued).

Composition(16)	%
Barium nitrate	<i>x</i>
Magnesium	<i>y</i>
Shellac	10

No.	<i>x</i> %	<i>y</i> %	$\Delta(\text{g/cm}^3)$	ν (s)	<i>T</i> (K)
H13	60	30	1.42	3.25	2,975
H14	45	45	1.30	5.25	2,825
H15	30	60	1.13	8.88	?
H16	15	75	1.03	did not burn	

Table 12. The Effects of Compositions Other Than in Table 11.

Composition (17)	%
Potassium perchlorate	<i>x</i>
Magnesium	<i>y</i>
Polyvinyl chloride	<i>z</i>

No.	<i>x</i> %	<i>y</i> %	<i>z</i> %	$\Delta(\text{g/cm}^3)$	ν (s)	<i>T</i> (K)
H25	45	45	10	1.2	3.58	3,260
H26	50	50	—	1.29	7.62	3,850

Composition (18)	%
Strontium nitrate	<i>x</i>
Magnesium	<i>y</i>
Polyvinyl chloride	<i>z</i>

No.	<i>x</i> %	<i>y</i> %	<i>z</i> %	$\Delta(\text{g/cm}^3)$	ν (s)	<i>T</i> (K)
H31	45	45	10	0.92	6.49	3,175
H28	50	50	—	1.17	9.30	?

Table 12. The Effects of Compositions Other Than in Table 11 (Continued).

Composition (19)	%
Barium nitrate	<i>x</i>
Magnesium	<i>y</i>
Polyvinyl chloride	<i>z</i>

No.	<i>x</i> %	<i>y</i> %	<i>z</i> %	$\Delta(\text{g/cm}^3)$	ν (s)	<i>T</i> (K)
H29	45	45	10	1.25	6.81	2,990?
H30	50	50	—	1.41	24.0	3,775

Note: In general, high temperature flame compositions that contained magnesium did not burn smoothly without an organic fuel like shellac. Even when the composition contained 10% shellac, it did not burn smoothly except between 60–30% magnesium, producing many sparks.

Adding a sodium source to the sample compositions was unnecessary, because at high temperatures the Na–D lines always appeared clearly from impurities in the ingredients.

6.3 Examinations of the Results

(1) The effects of oxidizers

Comparing the effect at the same fuel to oxidizer ratio, strontium nitrate gave the highest temperature of all, followed by potassium perchlorate, barium nitrate, ammonium perchlorate, and potassium nitrate.

(2) The effects of the ratio of oxidizer to magnesium

In this experiment, the smaller the ratio of oxidizer to magnesium, the higher the temperature. This is a tendency that comes from the oxygen balance. Namely when the quantity of the magnesium is too large relative to the oxidizer, part of the magnesium is in a vapor state at the flame measuring point.

(3) The effects of fuels other than magnesium

Shellac or polyvinyl chloride were used. Polyvinyl chloride gave higher flame temperatures than shellac.

On the other hand, without any organic fuel, the burn rate of the sample increased to two or three times as large as that with organic fuels, and the temperatures rose to 3700–3800 K. That is, even when a small quantity of organic fuels, other than magnesium, is added to the high temperature composition, the temperatures of the flame decrease remarkably, and the burn rate also decreases.

VII. Conclusion

For low-temperature, colored-flame compositions that contained ordinary organic fuels and for the high temperature compositions that contained magnesium, the flame temperatures were measured by the line-reversal method using the Na–D lines.

The effects of oxidizers, fuels, color agents and the ratios of those components on flame temperatures were examined, and the fundamental data necessary for spectral analysis were obtained.

For high temperature flames, a photographic method was used to obtain the intensities of the spectra. Therefore some errors were unavoidable due to the operation and the instability of the flames. The flames move or oscillate with time; so it will be desirable to use a device to shorten the measurement time in the future.

Acknowledgment

The author thanks Professor Y. Yamamoto, Tokyo University, for his encouragement; Dr. Ryohei Ishida, the Institute of Industry, Tokyo, who kindly taught me about the line-reversal method; and Mr. Mamoru Nonaka, Institute of Electrical Technology, Tokyo, who gave me the data for the emissivity of tungsten.

References

- 1) Jiro Oishi, *Temperatures and Methods of Measurement* (1954) p 174.
- 2) Yoshiichi Omoto and Iwao Honjo, *Lightning and Electric Heat* (1956) p 9.
- 3) *ibid.* of (1), p 184.
- 4) *ibid.* of (1), p 182 and 183.
- 5) *ibid.* of (2), p 27.
- 6) Ryohei Ishida, "Temperature Measurement of Flame Light Source Using Line-Reversal Method", *Report of Institute of Industry, Tokyo*, **51** (1956) p 333 First Report.
- 7) J. C. De Vos, "A New Determination of the Emissivity of Tungsten Ribbon", *Physica*, **10** (1954) p 690.
- 8) Takeo Shimizu, "Studies on Colored Flame Compositions of Fireworks, Part I" *Journal of Industrial Explosives, Japan*, **19**, No.1 (1958) p 316.
- 9) *ibid.* (8).
- 10) *Fireworks, Hanabi*, (1947) p 200.